10710 *Inorg. Chem.* **2010**, *49*, 10710–10717
DOI: 10.1021/ic101906u

Inorganic Chemistry
Article

Reinvestigation of the M^{II} (M = Ni, Co)/TetraThiafulvaleneTetraCarboxylate System Using High-Throughput Methods: Isolation of a Molecular Complex and Its Single-Crystal-to-Single-Crystal Transformation to a Two-Dimensional Coordination Polymer

Thi Le Anh Nguyen,[†] Thomas Devic,[*,†] Pierre Mialane,[†] Eric Rivière,[‡] Andreas Sonnauer,[§] Norbert Stock,[§] Rezan Demir-Cakan,[∥] Mathieu Morcrette,[∥] Carine Livage,[†] Jérome Marrot,[†] Jean-Marie Tarascon,[∥] and Gérard Férey[†]

[†]*Institut Lavoisier, UMR CNRS 8180, Université de Versailles Saint-Quentin-en-Yvelines, 45 avenue des Etats-Unis, 78035 Versailles cedex, France,* [‡]*Institut de Chimie Moléculaire et des Matériaux d'Orsay, UMR CNRS 8182, Université Paris-Sud, 91405 Orsay Cedex, France,* [§]*Institut für Anorganische Chemie, Christian-Albrechts-Universität, Max-Eyth Str., 24118 Kiel, Germany, and* [∥]*LRCS UMR CNRS 6007, Université de Picardie Jules Verne, 33 rue Saint-Leu, 80039 Amiens, France*

Received September 17, 2010

A high-throughput methodology combined with X-ray powder diffraction measurements was used to investigate the reactivity of the TetraThiaFulvalene TetraCarboxylic acid ((TTF-TC)H_4) with divalent metals (M = Ni, Co) under various reaction conditions (stoichiometry, pH, temperature). Two new crystalline phases were identified and then studied by single crystal X-ray diffraction. Whereas the first one appears to be a simple salt, the second one, formulated $\{[M(H_2O)_4]_2(TTF\text{-}TC)\}\cdot 4H_2O$, is built of 2:1 M:TTF-TC molecular complexes and labeled **MIL-136**(Ni, Co) (MIL stands for Materials Institute Lavoisier). The combination of thermogravimetric analysis and thermodiffraction studies reveals that **MIL-136**(Ni) exhibits a complex dehydration behavior. Indeed, a partial dehydration/rehydration process led to the single-crystal-to-single-crystal transformation of the molecular compound in a two-dimensional coordination polymer formulated $\{[Ni_2(H_2O)_5(TTF\text{-}TC)]\}\cdot H_2O$ (**MIL-136′**(Ni)). Magnetic and redox properties of **MIL-136**(Ni, Co) were investigated. Magnetic measurements indicate that all the magnetic coupling, intra- and intermolecular, are very weak; thus, the magnetic data of **MIL-136**(Ni, Co) have been interpreted in term of single-ion spin orbit coupling. Solid state cyclic voltammetry of **MIL-136**(Ni, Co) presents three reversible waves which were assigned to the redox activity of the TTF core and the metallic cations. In contrast to solids based on TTF linkers and alkaline ions, the **MIL-136**(Ni, Co) complexes do not act as excellent positive electrode materials for Li batteries, but present two reversible electron oxidation of the TTF core. These observations were tentatively related to the strength of the metal-carboxylate bond.

Introduction

One of the noticeable advantages of Porous Coordination Polymers (PCPs) or Metal Organic Frameworks (MOFs),[1] compared to their purely inorganic counterparts is the chemical versatility offered by the presence of the organic moieties. Indeed, variation of the organic linkers allows for example (i) the control of the pore size,[2,3] (ii) the fine-tuning of the polarity and acidobasicity of the pore surface through the grafting of functional organic groups,[3,4] (iii) the introduction of reactive groups for postsynthesis functionalization,[5] or (iv) the addition of physical properties (optical,[6] magnetic,[7,8] redox.[9−15]) related

*To whom correspondence should be addressed. E-mail: devic@chimie.uvsq.fr.

(1) See for example the special issue: *Chem. Soc. Rev.* **2009**, *38*, 1201−1507, and references therein.

(2) Lin, X.; Jia, J.; Zhao, X.; Thomas, K. M.; Blake, A. J.; Walker, G. S.; Champness, N. R.; Hubberstey, P.; Schröder, M. *Angew. Chem., Int. Ed.* **2006**, *45*, 7358–7364.

(3) Eddaoudi, M.; Kim, J.; Rosi, N.; Vodak, D.; Wachter, J.; O'Keeffe, M.; Yaghi, O. M. *Science* **2002**, *295*, 469–472.

(4) Devic, T.; Horcajada, P.; Serre, C.; Salles, F.; Maurin, G.; Moulin, B.; Heurtaux, D.; Clet, G.; Vimont, A.; Grenèche, J.-M.; Le Ouay, B.; Moreau, F.; Magnier, E.; Filinchuk, Y.; Marrot, J.; Lavalley, J.-C.; Daturi, M.; Férey, G. *J. Am. Chem. Soc.* **2010**, *132*, 1127–1136.

(5) Wang, Z.; Cohen, S. M. *Chem. Soc. Rev.* **2009**, *38*, 1315–1329, and references therein.

(6) Allendorf, M. D.; Bauer, C. A.; Bhakta, R. K.; Houk, R. J. T. *Chem. Soc. Rev.* **2009**, *38*, 1330–1352 and references therein.

(7) Maspoch, D.; Ruiz-Molina, D.; Wurst, K.; Domingo, N.; Cavallini, M.; Biscarini, F.; Tejada, J.; Rovira, C.; Veciana, J. *Nat. Mater.* **2003**, *2*, 190–195.

(8) Pardo, E.; Ruiz-García, R.; Cano, J.; Ottenwaelder, X.; Lescouëzec, R.; Journaux, Y.; Lloret, F.; Julve, M. *Dalton Trans.* **2008**, 2780–2805, and references therein.

Published on Web 10/22/2010

to the core of the linker. In the latter case, the preparation of redox-active MOFs is of special interest, as it could lead to enhanced hydrogen storage,[11−14] electronic conductivity,[16−18] or open new perspectives such as the use of coordination polymers as positive electrodes for a lithium ion battery.[9,10,15,19,20] In most cases, the redox-active linkers used up to now are built up from carbon, hydrogen, oxygen, and sometimes nitrogen. Alternatively, the TetraThiaFulvalene (TTF, $C_6H_4S_4$), a sulfur rich conjugated core, is known to present two reversible and easily accessible oxidation states, and when crystallized in a mixed-valence state, able to give rise to conductive or superconductive organic molecular solids.[21] Numerous coordination complexes based on TTFs bearing neutral coordination groups (N, S, P) have been reported,[22] mainly with the final aim at synergistically combining in the resulting materials the effects of the unpaired electrons of the TTF core and the metallic cations (M).[23−26] On the other side, coordination compounds built up from carboxylate binding sites are far less common: molecular complexes or low dimensional coordination polymers (one-dimensional (1-D) or two-dimensional (2-D)) based either on TTF monocarboxylate (M = Rh,[27] Gd[28]) or dicarboxylate (M = Ni, Co,[29] Mg, Ca,[30] Na[31]) were reported. In the present work, we focus our attention on the highly symmetric TTF-tetracarboxylate linker ((TTF-TC)H_4, ($C_{10}H_4O_8S_4$), see Scheme 1).

Scheme 1. TetraCarboxylic TetraThiafulavene (TTF-TC)H_4 Used in the Present Study

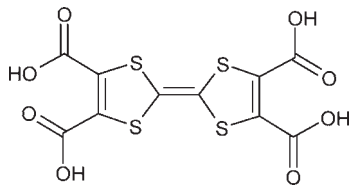

We recently showed that upon reaction with alkali salts (M = K, Rb, Cs), (TTF-TC)H_4 gives rise to three-dimensional (3-D) coordination polymers, which act as efficient positive electrode materials for lithium ion batteries.[32] Few coordination polymers with either Zn, Cu, or Mn and a neutral co-ligand (4,4′-bipyridine, 2,2′-bipyridine, phenanthroline) were also reported.[33,34] The reactivity of (TTF-TC)H_4 with Co(II) in water was also studied by Kepert et al. The resulting salt is built up from the isolated ionic species (TTF-TC)H_2^{2-} and $Co(H_2O)_6^{2+}$ linked through a 3-D framework of hydrogen bonds, and reversibly absorbs water.[35] More recently, Han et al. reported another salt, built up from (TTF-TC)H_2^{2-} anions and $Co_2(\mu_2\text{-}OH)_2(H_2O)_8^{2+}$ cations.[36] In both cases, no metal-carboxylate coordination bond was observed, what can at a first sight appear surprising, as carboxylate groups are known to react easily with divalent cations. We therefore decided to reinvestigate the TTF-TC/M^{II} (M = Ni, Co) system using a high-throughput (HT) methodology. Through the miniaturization and parallelization of the reactors, this technique allows the rapid screening of reaction conditions (stoichiometry, pH, nature of the solvent, temperature, and so forth), using a minimum amount of reactants. This is of particular interest when one of the reactants (such as (TTF-TC)H_4) requires a multistep synthesis. Recently applied to MOFs syntheses, the HT methodology allows at the same time (i) to discover new phases, (ii) to determine their domain of existence (of special interest when multiple phases coexist), and (iii) to optimize their synthesis (yield).[37−47] The HT methodology was thus applied to the (TTF-TC)H_4/(Co^{II}, Ni^{II}) system. The first part of this article is devoted to this HT investigation, especially to the isolation of the molecular coordination compound

(9) Armand, M.; Grugeon, S.; Vezin, H.; Laruelle, S.; Ribière, P.; Poizot, P.; Tarascon, J.-M. *Nat. Mater.* **2009**, *8*, 120–125.
(10) Chen, H.; Armand, M.; Courty, M.; Jiang, M.; Grey, C. P.; Dolhem, F.; Tarascon, J.-M.; Poizot, P. *J. Am. Chem. Soc.* **2009**, *131*, 8984–8988.
(11) Cheon, Y. E.; Suh, M. P. *Angew. Chem., Int. Ed.* **2009**, *48*, 2899–2903.
(12) Mulfort, K. L.; Hupp, J. T. *J. Am. Chem. Soc.* **2007**, *129*, 9604–9605.
(13) Mulfort, K. L.; Hupp, J. T. *Inorg. Chem.* **2008**, *47*, 7936–7938.
(14) Mulfort, K. L.; Wilson, T. M.; Wasielewski, M. R.; Hupp, J. T. *Langmuir* **2009**, *25*, 503–508.
(15) Xiang, J.; Chang, C.; Li, M.; Wu, S.; Yuan, L.; Sun, J. *Cryst. Growth Des.* **2008**, *8*, 280–282.
(16) Takaishi, S.; Hosoda, M.; Kajiwara, T.; Miyasaka, H.; Yamashita, M.; Nakanishi, Y.; Kitagawa, Y.; Yamaguchi, K.; Kobayashi, A.; Kitagawa, H. *Inorg. Chem.* **2009**, *48*, 9048–9050.
(17) Kobayashi, Y.; Jacobs, B.; Allendorf, M. D.; Long, J. R. *Chem. Mater.* **2010**, *22*, 4120–4122.
(18) Lopez, N.; Zhao, H.; Ota, A.; Prosvirin, A. V.; Reinheimer, E. W.; Dunbar, K. R. *Adv. Mater.* **2010**, *22*, 986–989.
(19) Fateeva, A.; Horcajada, P.; Devic, T.; Serre, C.; Marrot, J.; Grenèche, J.-M.; Morcrette, M.; Tarascon, J.-M.; Maurin, G.; Férey, G. *Eur. J. Inorg. Chem.* **2010**, 3789–3794.
(20) Férey, G.; Millange, F.; Morcrette, M.; Serre, C.; Doublet, M.-L.; Grenèche, J.-M.; Tarascon, J.-M. *Angew. Chem., Int. Ed.* **2007**, *46*, 3259–3263.
(21) See, for example the special issue on Molecular Conductors: *Chem. Rev.* **2004**, *104*, 4887−5782, and references therein.
(22) Lorcy, D.; Bellec, N.; Fourmigué, M.; Avarvari, N. *Coord. Chem. Rev.* **2009**, *253*, 1398–1438, and references therein.
(23) Hervé, K.; Le Gal, Y.; Ouahab, L.; Golhen, S.; Cador, O. *Synth. Met.* **2005**, *153*, 461–464.
(24) Liu, S. X.; Ambrus, C.; Dolder, S.; Neels, A.; Decurtins, S. *Inorg. Chem.* **2006**, *45*, 9622–9624.
(25) Lu, W.; Zhang, Y.; Dai, J.; Zhu, Q.-Y.; Bian, G.-Q.; Zhang, D.-Q. *Eur. J. Inorg. Chem.* **2006**, 1629–1634.
(26) Setifi, F.; Ouahab, L.; Golhen, S.; Yoshida, Y.; Saito, G. *Inorg. Chem.* **2003**, *42*, 1791–1793.
(27) Ebihara, M.; Nomura, M.; Sakai, S.; Kawamura, T. *Inorg. Chim. Acta* **2007**, *360*, 2345–2352.
(28) Pointillart, F.; Le Gal, Y.; Golhen, S.; Cador, O.; Ouahab, L. *Chem. Commun.* **2009**, 3777–3779.
(29) Gu, J.; Zhu, Q.-Y.; Zhang, Y.; Lu, W.; Niu, G.-Y.; Dai, J. *Inorg. Chem. Commun.* **2008**, *11*, 175–178.
(30) Wang, J.-P.; Lu, Z.-J.; Zhu, Q.-Y.; Zhang, Y.-P.; Qin, Y.-R.; Bian, G.-Q.; Dai, J. *Cryst. Growth Des.* **2010**, *10*, 2090–2095.
(31) Zhu, Q.-Y.; Lin, H.-H.; Dai, J.; Bian, G.-Q.; Zhang, Y.; Lu, W. *New J. Chem.* **2006**, *30*, 1140–1144.
(32) Nguyen, T. L. A.; Demir-Cakan, R.; Devic, T.; Morcrette, M.; Ahnfeldt, T.; Auban-Senzier, P.; Stock, N.; Goncalves, A.-M.; Filinchuk, Y.; Tarascon, J.-M.; Férey, G. *Inorg. Chem.* **2010**, *49*, 7135–7143.
(33) Han, Y.-F.; Li, X.-Y.; Li, J.-K.; Zheng, Z.-B.; Wu, R. T.; Lu, J.-R. *Chin. J. Inorg. Chem.* **2009**, *25*, 1290–1294.
(34) Qin, Y.-R.; Zhu, Q.-Y.; Huo, L.-B.; Shi, Z.; Bian, G.-Q.; Dai, J. *Inorg. Chem.* **2010**, *49*, 7372–7381.
(35) Kepert, C. J.; Hesek, D.; Beer, P. D.; Rosseinsky, M. J. *Angew. Chem., Int. Ed.* **1998**, *37*, 3158–3160.
(36) Han, Y.-F.; Li, M.; Wang, T.-W.; Li, Y.-Z.; Shen, Z.; Song, Y.; You, X.-Z. *Inorg. Chem. Commun.* **2008**, *11*, 945–947.
(37) Bauer, S.; Bein, T.; Stock, N. *Solid State Sci.* **2008**, *10*, 837–846.
(38) Bauer, S.; Stock, N. *Angew. Chem., Int. Ed.* **2007**, *46*, 6857–6860.
(39) Sonnauer, A.; Stock, N. *Eur. J. Inorg. Chem.* **2008**, *32*, 5038–5045.
(40) Sonnauer, A.; Stock, N. *J. Solid State Chem.* **2008**, *181*, 3065–3070.
(41) Biemmi, E.; Christian, S.; Stock, N.; Bein, T. *Microporous Mesoporous Mater.* **2009**, *117*, 111–117.
(42) Stock, N.; Bein, T. *J. Mater. Chem.* **2005**, *15*, 1384–1391.
(43) Forster, P. M.; Stock, N.; Cheetham, A. K. *Angew. Chem., Int. Ed.* **2005**, *44*, 7608–7611.
(44) Contreras, D.; Moreno, Y.; Salgado, Y.; Cardenas, G.; Baggio, R.; Pena, O.; Pivan, J. Y. *New. J. Chem.* **2007**, *31*, 1751–1754.
(45) Bauer, S.; Serre, C.; Devic, T.; Horcajada, P.; Marrot, J.; Férey., G.; Stock, N. *Inorg. Chem.* **2008**, *47*, 7568–7576.
(46) Banerjee, R.; Phan, A.; Wang, B.; Knobler, C.; Furukawa, H.; O'Keeffe, M.; Yaghi, O. M. *Science* **2008**, *319*, 939–943.
(47) Stock, N. *Microporous Mesoporous Mater.* **2010**, *129*, 287–295.

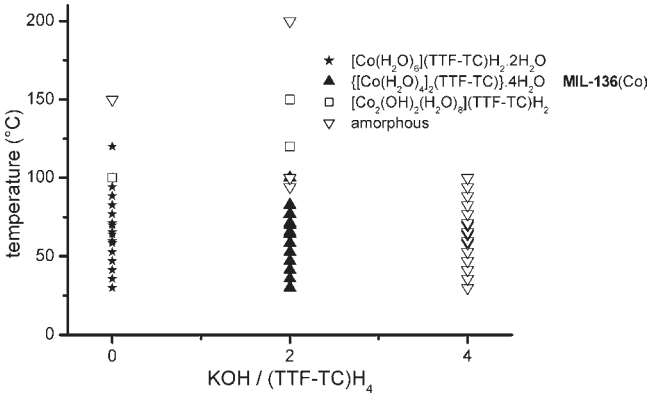

Figure 1. Results of the HT screening for the Co/(TTF-TC)H_4 system: effect of the temperature and pH.

(**MIL-136**(Ni, Co)). The second part is devoted to the structural and thermal behavior of this solid. We show that upon a dehydration/rehydration process, **MIL-136**(Ni) evolves to a 2-D coordination polymer **MIL-136′**(Ni) in a single-crystal-to-single-crystal process. Finally, the magnetic and electrochemical properties of **MIL-136**(Ni,Co) are presented.

Experimental Section

Synthesis. The TetraThiaFulvaleneTetraCarboxylic acid or (TTF-TC)H_4 was prepared in four steps following the published procedure.[32,48] The experimental parameters (temperature, pH) leading to the formation of $\{[Co(H_2O)_4]_2(TTF\text{-}TC)\}\cdot 4H_2O$ or **MIL-136**(Co) were determined using the HT methodology. These experiments, as well as the optimized experimental conditions used for the preparation of **MIL-136**(Co) and **MIL-136**(Ni) at a larger scale, are described in detail in the Supporting Information.

Characterizations. The Supporting Information contains the details of the different techniques (single crystal and powder X-ray diffraction (XRD), thermal analyses (TGA, thermodiffractometry), Infra-Red spectroscopy, magnetism, solid state electrochemistry) used for the characterization of the solids.

Results and Discussion

HT Synthesis and Structure. Previous studies suggested that water is an appropriate solvent for studying the reactivity of (TTF-TC)H_4.[32,35,36] The HT screening was thus performed with this solvent, (TTF-TC)H_4 and $Co(NO_3)_2\cdot 6H_2O$ as reactants, and using grids of 48 reactors with V_{max} = 0.25 mL. The resulting products were identified by powder XRD. Three experimental parameters were investigated: the temperature, the pH, and the TTF-TC/Co(II) ratio; only the first ones were found to be relevant (see Supporting Information, Tables S1 to S3). Variation of these parameters in the 20−150 °C and KOH/(TTF-TC)H_4 = 0−2 ranges lead to three crystalline phases, whereas higher temperature or pH only afford amorphous solids (Figure 1), presumably issued from the destruction of the linker.

The low temperature/low pH phase corresponds to $[Co(H_2O)_6](TTF\text{-}TC)H_2\cdot 2H_2O$, the salt already reported by Kepert et al.[35] Increasing the temperature (and eventually the pH) lead to a second phase, for which crystals of rather poor quality were obtained. Single-crystal XRD measurements nevertheless allowed a reasonably good structural model, indicating that this solid is again a salt, built up from $(TTF\text{-}TC)H_2^{2-}$ anions and $Co_2(\mu_2\text{-}OH)_2(H_2O)_8^{2+}$ cations (see Supporting Information, Figure S8). This compound is thus similar to the one reported by Han et al.[36] Finally, the third compound, isolated at intermediate pH (KOH/(TTF-TC)H_4 = 2) and low temperature (< 100 °C), was also identified by single-crystal XRD measurements. It is formulated $\{[Co(H_2O)_4]_2(TTF\text{-}TC)\}\cdot 4H_2O$ (later labeled **MIL-136**(Co), see Figure 2a), and consists of symmetrical 1:2 $TTF\text{-}TC^{4-}/Co^{2+}$ molecular complexes (Figure 2c). Using identical experimental conditions with Co(II) and Ni(II) but at a larger scale (24 mL Parr bomb) lead to the isotypic compounds **MIL-136**(M) (M = Ni, Co), as checked by powder XRD (see Supporting Information, Figure S1).

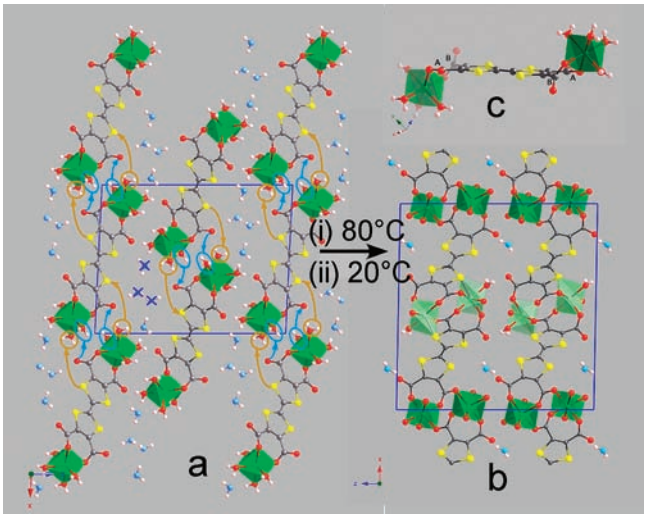

Figure 2. (010) projections at the same scale of the structures of **MIL-136**(Ni) (a) and **MIL-136′**(Ni) (b); (color code: Ni, green; O, red; S, yellow; H, white; O of free water molecules, pale blue). In (a) are highlighted within ellipses (blue), circles (orange), and crosses (dark blue) the water molecules (either bound or free) which leave the structure during the partial dehydration to give rise to **MIL-136′**(Ni) (see text). (c) The neutral $[M(H_2O)_4]_2(TTF\text{-}TC)$ (M = Co, Ni) molecular complex in **MIL-136**(M).

The neutral building unit in both **MIL-136** and **MIL-136′** (see below) structures corresponds to a fully deprotonated $TTF\text{-}TC^{4-}$ linker acting as chelating agent for the M^{II} cation on both sides (Figure 2c). In **MIL-136**, the coordination sphere of M^{II} is completed by four water molecules. In the resulting octahedral geometry, M^{II}−O distances and angles are in the usual range (Co−O = 2.069(5)−2.124(5) Å, Ni−O = 2.038(2)−2.060(2) Å). The TTF core is planar, and internal C=C and C−S bond distances indicate that the TTF remains in its reduced state, in accordance with the formulation (see Supporting Information, Tables S7 and S8 for TTF characteristics and bond valence calculations respectively). At each side, one carboxylate group (noted A in Figure 2c) lies in the plane of the TTF molecule, whereas the other one is twisted (angles between the TTF and the CO_2 planes = 7.8(4) and 63.7(5)°, and 7.1(1) and 62.4(2)° for **MIL-136**(Co) and **MIL-136**(Ni), respectively). The 2:1 complexes stacks parallel to each other (TTF-TTF interplane distance = 3.509(5) Å, see Supporting Information, Figure S11) but staggered, all the stacks being also parallel to each other (Figure 2a), finally defining pockets in which the free water molecules stand. Dangling oxygen atoms from the carboxylate groups and both bound and free water

(48) Pittman, C. U.; Narita, M.; Liang, Y. F. *J. Org. Chem.* **1976**, *41*, 2855–2860.

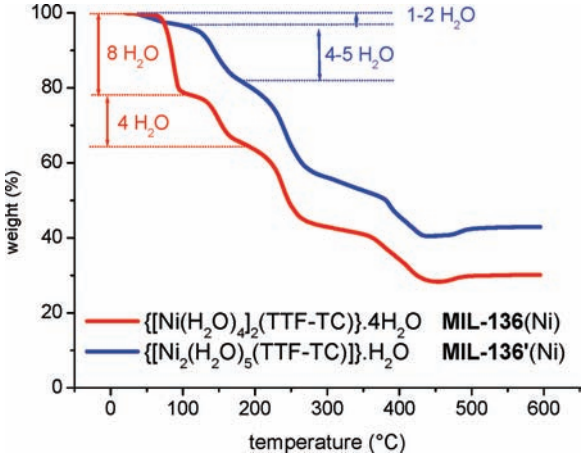

Figure 3. Thermogravimeric analysis of **MIL-136**(Ni) and **MIL-136′**-(Ni) under O_2.

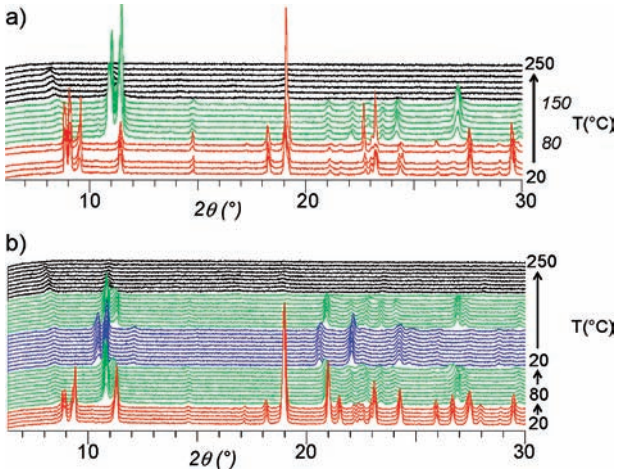

Figure 4. X-ray thermodiffractogram of **MIL-136**(Ni) under air (10 °C step). (a) From 20 to 250 °C; (b) from 20 to 80 °C and from 20 to 250 °C. Red, $\{[Ni(H_2O)_4(TTF\text{-}TC)]_2\}\cdot 4H_2O$ or **MIL-136**(Ni); blue, $\{[Ni_2(H_2O)_5(TTF\text{-}TC)]\}\cdot H_2O$ or **MIL-136′**(Ni); green, $\{[Ni_2(H_2O)_4(TTF\text{-}TC)]\}$.

Scheme 2. Water Adsorption/Desorption Process in **MIL-136**(Ni)

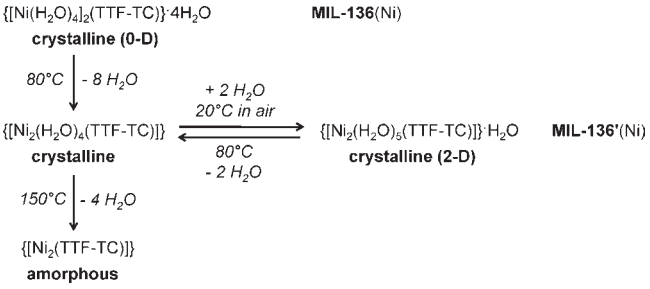

molecules lead to a complex 3-D hydrogen bond network. High quality XRD data for M = Ni allowed the location of the H atoms by Fourier difference. It reveals that the four independent O atoms from the carboxylate (O_{car}, coordinated or not) act as either one-, two-, or three- fold hydrogen bond acceptors ($H\cdots O_{car}$ = 1.92(5)−2.27(3) Å, $O(-H)\cdots O_{car}$ = 2.724(3)−2.988(3) Å, $O-H\cdots O_{car}$ = 150(4)−171(3)°, see Supporting Information, Table S5 for full details), connecting the complexes in the 101 plane. Both free water molecules acts as dihydrogen bond donors and acceptors, with almost ideal $H\cdots O-H$ angles (99(3)−127(2)°). In contrast, bound water molecules act mainly as hydrogen bond donors.

As shown earlier, the pH seems to play a major role in the formation of a metal complex. One can nevertheless note that Kepert et al.,[35] using diffusion in silica gel and basic conditions, only observed the above-mentioned salt, which may be a consequence of a heterogeneous pH in their medium. The formation of a metal complex requires an intermediate pH, but, as a consequence of the low temperature, only a low-dimensional metal complex (i.e., a *molecular* complex) was formed.[49] These results suggest that getting a higher dimensionality (preferably 3-D) would require a drastic change of the experimental conditions (not only temperature), such as the nature of the solvent, which was not explored in the present study.

Thermal Behavior and Single-Crystal-to-Single-Crystal Transformation. The thermal behavior of **MIL-136**(Ni) (see Supporting Information, Figures S2 and S4 for **MIL-136**(Co)) was examined by thermogravimetric analysis under oxygen (Figure 3) and thermodiffraction under air (Figure 4). These studies first indicate that this solid is stable up to 150 °C and loses its crystallinity above this temperature. At lower temperature (80 °C), a first weight loss, corresponding to the departure of 8 water molecules (experimental and theoretical weight losses are 21 and 20% respectively) is accompanied by a structural change (see Figure 4a the red and green diagrams). The second weight loss at 150 °C, associated with the complete dehydration of **MIL-136** (experimental and theoretical weight losses are 33 and 30% respectively) lead to an amorphous compound (see Figure 4 the green and black diagrams) which then collapse with the combustion of the organic moiety (see Figure 3).

In an attempt to isolate the lower hydrate $\{[Ni_2(H_2O)_4(TTF\text{-}TC)]\}$, corresponding to the loss of 8 water molecules, a sample of **MIL-136**(Ni) was heated up to 80 °C, and then cooled down to room temperature. As shown in Figure 4b, $\{[Ni_2(H_2O)_4(TTF\text{-}TC)]\}$, upon cooling, transforms into a new structural form (blue pattern), hereafter labeled **MIL-136′**(Ni) and formulated $\{[Ni_2(H_2O)_5(TTF\text{-}TC)]\}\cdot H_2O$ (see below). This transformation is reversible, as upon heating the previous pattern (green) is recovered. A thermogravimetric analysis indicates that this new solid **MIL-136′**(Ni) contain 6 water molecules, which are removed in two steps (2 + 4), in accordance with the behavior of **MIL-136**(Ni) (Figure 3). Scheme 2 summarizes the full dehydration/hydration process of **MIL-136**(Ni).

Description of the Structure of MIL-136′(Ni) and Study of the Structural Relations between MIL-136(Ni) and MIL-136′(Ni). Upon a slow heating at 80 °C followed by cooling at 20 °C, it was possible to isolate a single crystal of **MIL-136′**(Ni) suitable for XRD measurement. From the structure determination, the formula of **MIL-136′**(Ni) is $\{[Ni_2(H_2O)_5(TTF\text{-}TC)]\}\cdot H_2O$, in agreement with the TG analysis. The structure (Figure 2b) exhibits topological similarities with **MIL-136**(Ni) in terms of molecular building units, but also differences due to the loss of both free and bound water molecules which induce

(49) Forster, P. M.; Burbank, A. R.; Livage, C.; Férey, G.; Cheetham, A. K. *Chem. Commun.* **2004**, 368–369.

some important changes in the connectivity. The first striking feature which explains the latter is the rather unusual short distance (2.517 Å) which appears between Ni^{II} and some sulfur atoms of the TTF group, implying important atomic movements during the transition. Bond valence calculations (see Supporting Information, Table S8) confirm that these S belong to the coordination sphere of Ni, taking the place of one water molecule of the Ni octahedron. Simultaneously, by the departure of another framework water molecule, the previously dangling O atoms from the carboxylate groups become ligands of a Ni^{II} ion. These cooperative displacements, summarized by arrows and crosses in Figure 2a, have several consequences: (i) despite keeping the same global octahedral coordination, Ni^{II} ions segregate into two different crystallographic sites, reflecting their different neighborhoods, namely, $[NiO_3(H_2O)_3]$ and $[NiO_3S(H_2O)_2]$; (ii) 3/4 of the water molecules in the pockets (crosses in Figure 2a) disappear and (iii) the introduction of O and S from the TTF-TC into one Ni coordination makes that **MIL-136′**(Ni) exhibits now a 2-D dimensionality with layers developing along the 110 plane, by connection along [010] and [100] of the previously isolated and stacked molecular building units. Note that this condensation, which leads to some bending of the TTF cores (Supporting Information, Figure S12), is not associated with a redox process, as the oxidation state of both the metal and the TTF core remain unchanged (see Supporting Information, Tables S7 and S8). It is however surprising—and rather rare[50−58]—to observe that, despite these strong reorganizations, a single-crystal-to-single-crystal transformation occurs, involving a change of dimensionality (here from 0 to 2-D) upon the departure of bound solvent molecules.

Despite the failure to isolate the unstable $\{[Ni_2(H_2O)_4(TTF\text{-}TC)]\}$, which readily reabsorbs water to form **MIL-136′**(Ni) and therefore forbids any structural study, the knowledge of the structure of **MIL-136′**(Ni) allows us to anticipate this unknown structure. In terms of formulation, the two solids differ only by two water molecules. One can therefore imagine that one of them is the free H_2O observed in **MIL-136′**(Ni), the second belonging to one of the nickel octahedra of **MIL-136′**(Ni), likely on $[NiO_3S(H_2O)_2]$, the most distorted one. The disappearance of one H_2O in this species would generate a 5-fold, very distorted coordination for Ni, rendering this polyhedron very unstable by cooling, thus tentatively explaining the partial and topotactic rehydration into **MIL-136′**(Ni). The amorphous character of the fully dehydrated solid prohibits any structural expectation.

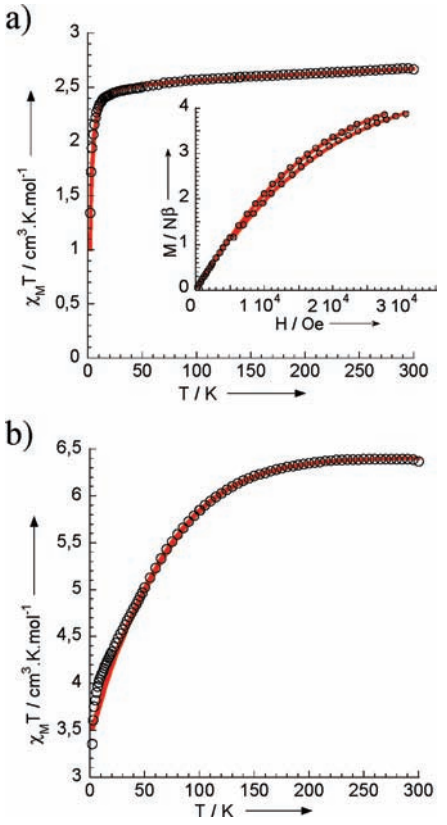

Figure 5. Magnetic susceptibility data in $\chi_M T$ form of (a) **MIL-136**(Ni) and (b) **MIL-136**(Co). The solid line above the experimental data is the theoretical curve derived from the Hamiltonian(3) and (4) respectively (see Supporting Information). Inset (a): magnetization versus magnetic field at 1.8 and 2 K for **MIL-136**(Ni). The solid lines represent the best fitting results using Hamiltonian(1) (see text).

Finally, in agreement with the dense character of the phases, no significant N_2 adsorption at 77 K was detected whatever hydration state was considered ($S_{BET} < 20\,m^2\,g^{-1}$, see Supporting Information).

Magnetic Properties. To determine if intra- and/or intermolecular magnetic interactions occur between the paramagnetic ions constituting the **MIL-136**(Ni) and **MIL-136**(Co) compounds, the magnetic properties of these two species have been studied.

The $\chi_M T$ versus T plot of **MIL-136**(Ni) is depicted in Figure 5a. The $\chi_M T$ product is nearly constant from room temperature ($\chi_M T = 2.67$ cm^3 K mol^{-1}) to about 20 K ($\chi_M T = 2.44$ cm^3 K mol^{-1}), and then decreases from 20 to 1.8 K ($\chi_M T = 1.34$ cm^3 K mol^{-1}). The smooth decrease from room temperature to 20 K can be attributed to the temperature-independent paramagnetism (TIP) of the Ni^{II} ions. The decrease at low temperature can be attributed to the zero-field splitting (zfs) effect, known to be significant for Ni^{II} ions,[59] and potential weak intra- and/or intermolecular magnetic exchanges.

First, the $1/\chi_M = f(T)$ curve has been fitted with the Curie−Weiss law $\chi_M = C/(T - \theta)$ (Supporting Information, Figure S5), affording $C = 1.27$ cm^3 mol^{-1} K (implying $g = 2.25$) and $\theta = -0.60$ K. Second, the magnetization

(50) Bradshaw, D.; Warren, J. E.; Rosseinsky, M. J. *Science* **2007**, *315*, 977–980.
(51) Campo, J.; Falvello, L. R.; Mayoral, I.; Palacio, F.; Soler, T.; Tomas, M. *J. Am. Chem. Soc.* **2008**, *130*, 2932–2933.
(52) Sadeghzadeh, H.; Morsali, A. *Inorg. Chem.* **2009**, *48*, 10871–10873.
(53) Mahmoudi, G.; Morsali, A. *Cryst. Growth Des.* **2008**, *8*, 391–394.
(54) Zhu, P.; Gu, W.; Zhang, L.-Z.; Liu, X.; Tian, J.-L.; Yan, S.-P. *Eur. J. Inorg. Chem.* **2008**, 2971–2974.
(55) Xue, D.-X.; Zhang, W. X.; Chen, X.-M.; Wang, H.-Z. *Chem. Commun.* **2008**, 1551–1553.
(56) Aslani, A.; Morsali, A. *Chem. Commun.* **2008**, 3402–3404.
(57) Ghosh, S. K.; Kaneko, W.; Kiriya, D.; Ohba, M.; Kitagawa, S. *Angew. Chem., Int. Ed.* **2008**, *47*, 8843–8847.
(58) Zhang, L.-Z.; Gu, W.; Liu, X.; Dong, Z.; Li, B. *CrystEngComm* **2008**, *10*, 652–654.
(59) Boca, R. *Coord. Chem. Rev.* **2004**, *248*, 757–815.

versus field curves (Figure 5a, inset) recorded at 1.8 and 2 K have been fitted considering the Hamiltonian(1):

$$\hat{H}(1) = \mu_B \hat{B} \cdot [g] \cdot \hat{S} + D(\hat{S}_z^2 - 1/3\hat{S}^2)$$

where D is the local axial zfs parameter. This affords $|D| = 4.9\ cm^{-1}$, g being fixed to 2.25 ($R = 1.1 \times 10^{-4}$, with $R = [\sum(M_{calc} - M_{obs})^2/\sum(M_{obs})^2]$). No improvement of the fit is obtained when an equatorial zfs parameter is introduced in $\hat{H}(1)$. These g and D values are well in the range of those previously reported for mononuclear nickel complexes. Moreover, such result is in perfect agreement with those previously obtained for octahedral Ni^{II} complexes coordinated to six oxygen atoms. We can mention for example that the $[Ni(H_2O)_6](SO_4)$ compound is characterized by $|D| = 4.9\ cm^{-1}$ and $g = 2.24$.[60] Moreover, attempts to fit the $\chi_M T = f(T)$ curve of **MIL-136**(Ni) considering a Heisenberg spin Hamiltonian have failed (see Supporting Information). Thus, in **MIL-136**(Ni), the nickel centers are pseudo isolated, with weak intermolecular antiferromagnetic interactions.

The magnetic properties of the **MIL-136**(Co) cobalt(II) complex have also been studied. The $\chi_M T = f(T)$ curve of **MIL-136**(Co) decreases continuously from room temperature ($\chi_M T = 6.80\ cm^3\ K\ mol^{-1}$) to 1.8 K ($\chi_M T = 3.57\ cm^3\ K\ mol^{-1}$), as shown Figure 5b. Before any interpretation of these data, it must be recalled that high-spin Co^{II} complexes in O_h symmetry possess a $^4T_{1g}$ ground state. This implies that the contribution of the orbital momentum cannot be ignored, complicating the theoretical analysis of the magnetic data.[61] Nevertheless, taking into account that **MIL-136**(Ni) and **MIL-136**(Co) are isostructural and the results reported above for **MIL-136**(Ni), we have considered a model where the Co^{II} centers are supposed to be magnetically isolated. Then, the data has been treated with the Hamiltonian(4):

$$\hat{H}(4) = \alpha\lambda\hat{L}\hat{S} + \Delta[\hat{L}_z^2 - 1/3\hat{L}^2]$$

where λ is the spin−orbit coupling parameter, α is the orbital reduction factor, and Δ reflects the degree of distortion of the Co^{II} octahedron. The magnetic data have thus been fitted considering the empirical equation developed by Lloret et al.[62] The best fit to the experimental data in the 20−300 K temperature range afforded $\lambda = -113\ cm^{-1}$ and $\Delta = 388\ cm^{-1}$, α being fixed to 1.5. The slight deviation at low temperature of the experimental curve to the calculated one can be attributed to the presence of weak antiferromagnetic interactions. In conclusion, in both **MIL-136**(Ni) and **MIL-136**(Co), the magnetic ions can be considered as pseudo-isolated paramagnetic centers, with weak antiferromagnetic interactions. As the shortest intermolecular Ni(II)···Ni(II) distances are almost equal for **MIL-136′**(Ni) (5.082(4) and 5.0380(5) Å for **MIL-136′**(Ni) and **MIL-136**(Ni), respectively), one can also assume the same behavior for the hemihydrated form.

Redox Activity. The cyclic voltammetry of (TTF-TC)H_4 in solution was shown to exhibit two oxidation waves characteristic of the TTF core;[32,35] nevertheless, only the first one was found to be reversible, a phenomenon which could be related to the decarboxylation of the linker in its dioxidized form.[32,63,64] Here, the low solubility of the complexes **MIL-136**(Ni) and **MIL-136**(Co) preclude their studies in solution. Therefore, electrochemical experiments were performed in the solid state, using **MIL-136**(Ni), **MIL-136′**(Ni), and **MIL-136**(Co) as positive electrode materials in a classical two-electrode Swagelok-type cell in which a metallic lithium foil was used as negative and reference electrode. Coordination polymers based on redox-active metal[19,20] or linkers[9,10] were indeed shown to act as reasonably good positive electrode materials for Li-ion batteries, a property requiring not only a reversible redox activity but also a good Li^+ mobility within the solid. The solid-state cyclic voltammogram (CV) experiments were performed between 2 and 4 V versus Li/Li^+ at 0.1 mV s^{-1} voltage sweep rate where three reversible redox couples were observed at about 2.50, 3.20, and 3.60 V for all solids (see Figure 6 for **MIL-136**(Ni,Co) and Supporting Information, Figure S7 for **MIL-136′**(Ni)).

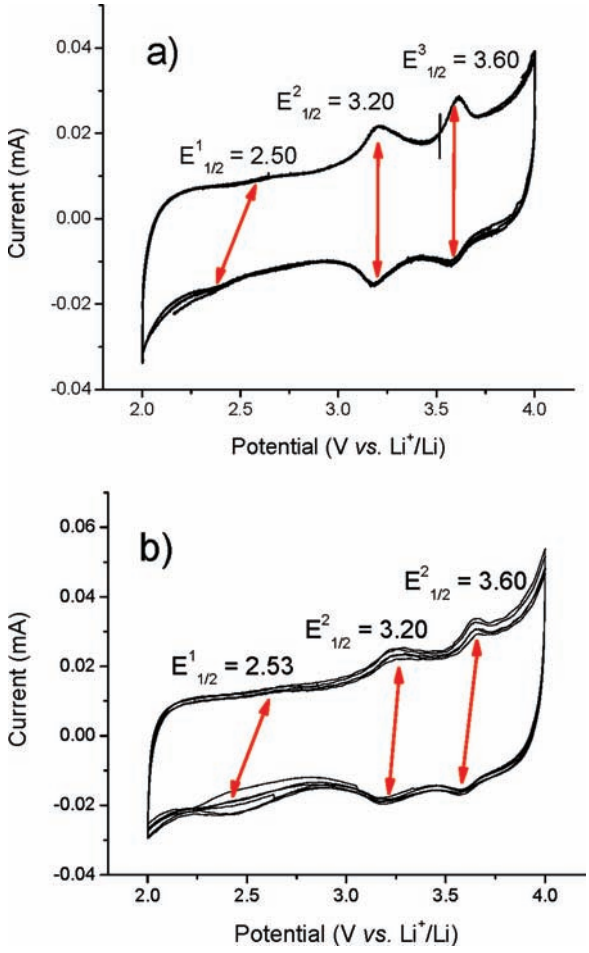

Figure 6. Solid-state cyclic voltammetry between the voltage range of 2 and 4 V versus Li/Li^+ at 0.1 mV s^{-1} sweep rate for (a) **MIL-136**(Ni) and (b) **MIL-136**(Co).

(60) Fisher, R. A.; Hornung, E. W. *J. Chem. Phys.* **1968**, *48*, 4284–4291.
(61) Kahn, O. *Molecular Magnetism*; VCH Publishers: New York, 1993.
(62) Lloret, F.; Julve, M.; Cano, J.; Ruiz-García, R.; Pardo, E. *Inorg. Chim. Acta* **2008**, *361*, 3432–3445.
(63) Dolbecq, A.; Fourmigué, M.; Batail, P. *Bull. Chem. Soc.* **1996**, *133*, 83–88.
(64) Idriss, K. A.; Chambers, J. Q. *J. Electroanal. Chem.* **1980**, *109*, 341–352.

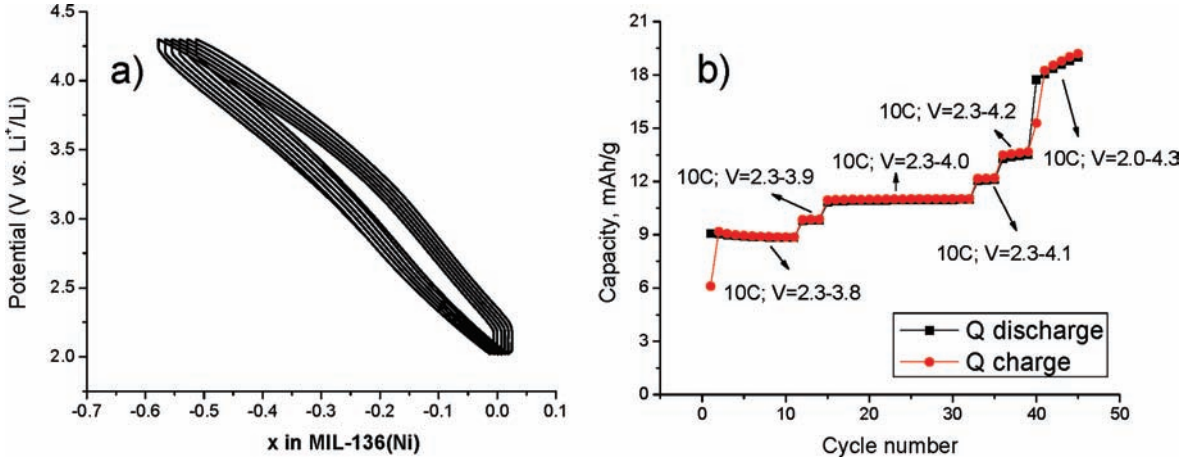

Figure 7. (a) Galvanostatic charge−discharge profile of **MIL-136**(Ni) at constant 10 C current density (which corresponds to the current required to completely charge/discharge an electrode in 6 min) for the voltage range between 2.0−4.3 V. (b) Rate performance of **MIL-136**(Ni) at 10 C current densities with different voltage ranges.

The half-wave potentials were tentatively assigned as follows: the two high-potential ones are related to the first and second oxidations of the TTF core ($E^2_{1/2}$ = 3.20 and $E^3_{1/2}$ = 3.60), and the low and very broad peak ($E^1_{1/2}$ = 2.50) to the reduction of the metallic cations ($M^{II} \rightarrow M^{I}$). The oxidation of the metal ($M^{II} \rightarrow M^{III}$), which should appear at high potential (> 4 V), is not observed here even if the voltage range was increased up to 4.5 V (see Supporting Information, Figure S7a for **MIL-136′**(Ni)). When scanning at lower voltage range (< 2 V), an irreversible reduction process occurred, which could be related to either the reduction of the metal ($M^{I} \rightarrow M^{0}$) or the water molecule (see Supporting Information, Figure S6). By comparison with the CVs of the **MIL-136**(Ni,Co) and M_2(TTF-TC)H_2 (M = K, Rb, Cs) solids,[32] two differences emerge: (i) the second oxidation of the TTF core appears reversible, and (ii) the general cycling behavior, in which **MIL-136**(Ni,Co) were able to charge at high voltage value (4.3 V) without having irreversible capacity loss. Figure 7a shows the fully reversible galvanostatic charge−discharge profile of **MIL-136**(Ni) at constant 10 C current density between the voltage range of 2.0−4.3 V (see Supporting Information, Figure S7b for **MIL-136′**(Ni)). The curve presents a typical solid solution reaction with capacity around 20 mAh/g (~0.6 e^- insertions). However at the same voltage range (2.3−3.7) and cycling rate (10 C) the reversible capacity of K_2(TTF-TC)H_2 was around 50 mAh/g (~0.6 e^- insertions)[32] at variance with **MIL-136**(Ni), < 9 mAh/g (~0.25 e^- insertions). Both differences could be tentatively related to the strength of the carboxylate-cation interaction. A reasonable activity as electrode materials for Li-ion battery requires a good ionic mobility as well as good lithium and electron delocalization. This is indeed the case for M = alkaline ions, where exchange between M^+ and Li^+ could occur,[32] but not for M = divalent cations, as these ones interact more strongly with the carboxylate groups. As a consequence, first **MIL-136**(Ni), **MIL-136′**(Ni), and **MIL-136**(Co) present a very limited charge capacity (~ 20 mA g^{-1} at 10 C regime between the voltage range of 2.0−4.3 V). Second, the second oxidation of the TTF core appears irreversible both in solution for (TTF-TC)H_4 and in the solid state for M_2(TTF-TC)H_2 (M = K, Rb, Cs), but reversible here. This unusual behavior is nevertheless in agreement with the recent publication by Qin et al. where they showed that Mn^{II} atoms linked to TTF-TC through carboxylate bridges resulted in two reversible redox couples.[34] A possible explanation could be that the combination of strong metal(II)-carboxylate interactions and structural rigidity may force the carboxylate groups to remain coordinated to the metal and thus close to the TTF core, preventing the decarboxylation; whereas for M_2(TTF-TC)H_2 (M = K, Rb, Cs), the metal-carboxylate bond is weaker and could not prevent the departure of CO_2 in the solid state.

Conclusion

We report here a coordination compound based on the $\{[M(H_2O)_4]_2(TTF\text{-}TC)\}\cdot 4H_2O$ (M = Ni, Co) unit. This molecular complex crystallizes with both bound and free water molecules, and exhibits a complex thermal behavior. Indeed, a partial dehydration−rehydration process allows the isolation of a 2-D coordination polymer, which results from the condensation of the above-mentioned complex. This transformation occurs in a single-crystal-to-single-crystal fashion. The magnetic and redox properties of these complexes were also investigated. Temperature and field dependent magnetic measurements first indicate that the divalent cations are pseudo-isolated, as almost no intra or intermolecular magnetic coupling was detected. Solid state electrochemistry shows that, contrary to the solids based on the same linker but alkaline ions, the $\{[M(H_2O)_4]_2(TTF\text{-}TC)\}\cdot 4H_2O$ (M = Ni, Co) complexes are not suitable candidates for use as positive electrodes for Li batteries, but exhibit an unexpected, fully reversible two electron oxidation process for the TTF core. These observations were tentatively related to the strength of the metal-carboxylate bond.

Although the use of the HT methodology allows the isolation of a new molecular complex, no 3-D framework structure could be obtained, certainly because of the rather mild conditions required by the organic ligand (in term of temperature and pH). Nevertheless, alternative synthetic approaches could be considered to circumvolve this limitation, such as (i) the use of a neutral co-ligand (4,4′-bipyridine or similar compounds) to connect the molecular species,[33,34]

or (ii) their controlled condensation by a careful dehydration process. Moreover, even if such solids seem not very effective as electrodes for Li batteries, their redox activity could be exploited alternatively. As an example, the partial oxidation of the TTF core either post-synthesis by reaction with an oxidant or during the synthesis by a combined electro-hydrothermal approach[32] could lead to conducting properties (as the one encountered in regular molecular TTF-based materials) or at least interactions between the unpaired electrons of the metallic cations and the radical TTF cores.[23−26,28] These research paths are currently explored in our laboratories.

Acknowledgment. The authors acknowledge the MENRT and the ANR for financial support (Ph.D. grant for T.L.A.N. and project "CONDMOFs" respectively), the ESRF for providing access to the beamline BM01A and Dr. Y. Filinchuk for his help during the synchrotron experiments.

Supporting Information Available: Full synthetic procedures and experimental details related to the characterization of the solids (powder and single crystal XRD, IR spectroscopy, thermogravimetric analysis, magnetic measurements, solid state electrochemistry). This material is available free of charge via the Internet at http://pubs.acs.org.